Journal of Comparative Neurology

WILEY

JCN RESEARCH IN SYSTEMS NEUROSCIENCE THE JOURNAL OF COMPARATIVE NEUROLOGY

RESEARCH ARTICLE OPEN ACCESS

The Brain of the African Wild Dog. V. The Somatosensory System and Vestibular Nuclear Complex

Samson Chengetanai[1] | Adhil Bhagwandin[1] | Mads F. Bertelsen[2] | Therese Hård[3] | Patrick R. Hof[4,5] | Muhammad A. Spocter[1,6] | Paul R. Manger[1]

[1]Department of Anatomical Sciences, Faculty of Health Sciences, University of the Witwatersrand, Parktown, South Africa | [2]Copenhagen Zoo, Frederiksberg, Denmark | [3]Borås Zoo, Borås, Sweden | [4]Nash Family Department of Neuroscience and Friedman Brain Institute, Icahn School of Medicine at Mount Sinai, New York, New York, USA | [5]New York Consortium in Evolutionary Primatology, New York, New York, USA | [6]Department of Anatomy, Des Moines University, Des Moines, Iowa, USA

Correspondence: Paul R. Manger (Paul.Manger@wits.ac.za)

Received: 14 April 2025 | **Revised:** 16 June 2025 | **Accepted:** 27 June 2025

Funding: This work was supported by funding from the South African National Research Foundation (P.R.M.), The Verizon Foundation (M.A.S.), and the Carnegie-Wits Alumni Diaspora Program through the Carnegie Corporation of New York (M.A.S. and P.R.M.).

Keywords: canids | Carnivora | neuroanatomy

ABSTRACT

Social behaviors in the African wild dog (*Lycaon pictus*) commonly involve a range of tactile aspects, including biting, pushing, embracing, mounting, face and muzzle licking, nose–chin and muzzle contact, paw placement, play fighting, and wrestling, supported by the vestibular system. We employed an array of architectural and immunohistochemical stains to provide a qualitative description of the somatosensory and vestibular systems in the brain of one representative African wild dog individual. The appearance of both systems does not appear to differ from that reported in other Carnivora. The six nuclei forming the vestibular system, and their relationship to each other and the incoming vestibular branch of the eighth cranial nerve, appear like those observed in many mammalian species. The location and appearance of the dorsal column nuclei, the trigeminal sensory column, the colliculi, somatosensory nuclei of the dorsal thalamus, and the five somatosensory cortical areas observed in the African wild dog are like those observed in the domestic dog and other Carnivora. This study of the somatosensory and vestibular systems of the African wild dog completes our series of studies describing the major sensory systems in the African wild dog brain. It appears reasonable to conclude that, at the systems level of analysis, no overt specializations of any of the sensory systems are present. Thus, the neural underpinnings of the complex sociality of the African wild dog may be supported by nonsensory neural systems, such as motor, neuromodulatory, limbic, or cognitive systems, or levels of organization like receptor expression patterns or connectivity.

1 | Introduction

African wild dogs (*Lycaon pictus*) are an endangered, canid, pack species that exhibit a highly social life history (Creel and Creel 2002). Significant aspects of the social structure of African wild dogs include the distinct male and female hierarchies as well as a cooperative breeding system (van den Berghe et al. 2019), like that observed in other canids (e.g., Berghänel et al. 2022). While olfactory, auditory, and visual signals play a significant role in the social milieu of the African wild dog, systems-level neuroanatomical studies have not revealed any overt specializations associated with these senses (Chengetanai, Tenley, et al. 2020; Chengetanai, Bhagwandin, et al., 2020a, 2020b, 2020c) in comparison to the domestic dog that may contribute to our

understanding of the neural basis of the social structure and behaviors observed in this canid. While social interactions can be modified with pheromonal interventions (van den Berghe et al. 2019), no specific specializations of the accessory olfactory system were noted (Chengetanai, Bhagwandin, et al. 2020a).

Detailed descriptions of the olfactory, auditory, and visual sensory systems have been provided (Chengetanai, Bhagwandin, et al. 2020a, 2020b, 2020c); however, the somatosensory system of the African wild dog has yet to be investigated. Behavioral studies of the African wild dog indicate that tactile stimuli, in addition to the broad array of functions associated with this system (e.g., Kaas 2012; ten Donkelaar et al. 2020), may play an important role in sociality in this species. The detection and interpretation of distinct and subtle tactile stimuli experienced by African wild dogs may be involved in (1) severe aggressive behaviors such as assaults and biting; (2) ritualized aggression such as pushing, embracing, and biting of the snout and scruff; (3) dominance behaviors, such as genital inspection, mounting, and face licking; (4) submissive behaviors, such as licking of the muzzle during active submission; (5) affiliative behaviors, such as muzzle licking, nose–chin contact, licking of fur, paw placement on head or back, muzzle contact during greetings, and lateral body rubbing; and (6) play behaviors, such as gentle fur biting and pushing with the nose to elicit play, and play fighting and wrestling (van den Berghe et al. 2019). While not being specifically involved in these tactile-based behaviors, all these behaviors will be supported by the vestibular system. Many of these social behaviors involving the sense of touch displayed by the African wild dog are similar to that observed in the domestic dog (e.g., Ward et al., 2008; McGreevy et al. 2013), indicating that it is likely that the organization of the somatosensory system in the African wild dog, in relation to sociality, will be similar to that observed in the domestic dog.

The somatosensory system has been studied in detail in several mammalian species (e.g., Kaas 2012; Sawyer 2017; ten Donkelaar et al. 2020), revealing a highly conserved systems-level organization spanning the most caudal aspects of the medulla oblongata through to the cerebral cortex. Here, we continue our systematic description of the brain of the African wild dog (Chengetanai, Tenley, et al. 2020; Chengetanai, Bhagwandin, et al. 2020a, 2020b, 2020c), outlining the organization of the somatosensory and vestibular systems in this species. The broad aim of these studies is to determine the neural underpinnings of sociality in the African wild dog, which to date have not revealed overt specializations of the olfactory, auditory, and visual systems that may contribute to sociality.

2 | Materials and Methods

2.1 | Specimens

Ten adult African wild dog brains were obtained from Borås Zoo, Sweden (see Chengetanai, Tenley, et al. [2020] for full details of animals, permits, collection, and treatment of tissue). Antemortem observations for all these animals revealed that they were in good health with no obvious neural deficits or behavioral abnormalities and were euthanized for population management reasons (Bertelsen 2018). While these animals were bred in captivity, they were housed in a large naturalistic enclosure (6250 m^2 outdoor area, 33 m^2 indoor area) in a sizeable pack (size of pack at time of sampling was 19 animals, comparable to the typical size observed in wild populations, which generally range from 10 to 40 animals; Claase et al. 2024) and exhibited all normal social behaviors. All animals were treated and used according to the guidelines of the University of the Witwatersrand Animal Ethics Committee (AESC No. 2012/53/01), which parallel those of the NIH for the care and use of animals in scientific experimentation. In the current study, the whole brain of one of these specimens (LP2, a male with a brain mass of 141.5 g) was sectioned, stained, and analyzed. While this study is primarily based on our observations from a single specimen, in a previous study, this specimen and five others underwent MR imaging (Chengetanai, Tenley, et al. 2020). When comparing the specimen used herein to these other MR-scanned brains, no differences in terms of overall morphology of the somatosensory and vestibular systems, at the level of MRI resolution, were noted. We thus assume that this specimen is representative of the species but acknowledge that the use of a single specimen may introduce error into the interpretation made and thus temper our observations and conclusions accordingly.

2.2 | Sectioning, Immunohistochemical Staining, Antibody Characterization, and Specificity

Prior to sectioning, the brain was allowed to equilibrate in 30% sucrose in 0.1 M PB at 4°C and then frozen in crushed dry ice and sectioned into 50-μm-thick coronal sections on a freezing microtome into a 1-in-20 series of sections. Consecutive series of sections were stained for Nissl and myelin and immunolabeled for neuronal nuclear marker (NeuN), choline acetyltransferase (ChAT), tyrosine hydroxylase (TH), parvalbumin (PV), calbindin (CB), calretinin (CR), neurofilament H (NFH), and vesicular glutamate transporter 2 (vGlut2). The remaining 10 series of sections were stored in an antifreeze medium for future use. The sections used for Nissl staining were mounted on 0.5% gelatine-coated glass slides, allowed to dry for 48 h, and cleared in a solution of 1:1 chloroform and 100% alcohol overnight. The sections were then hydrated in a graded series of alcohol (100%, 100%, 95%, 70%, and 50%), after which the sections were stained with 1% cresyl violet (Sigma–Aldrich, C5042, PubChem CID: 135445693). The sections were then washed in distilled water, treated in 50% alcohol to remove excess cresyl violet stain, differentiated in 70% alcohol with some added acetic acid, dehydrated in 95%, 100%, and 100% alcohol, cleared in xylene, and cover-slipped with Depex. The sections used for myelin staining were refrigerated for 2 weeks in 5% formalin, then mounted on 1.0% gelatine-coated slides, and stained with a modified silver stain (Gallyas 1979). Full details of the immunostaining protocol and the characterization and specificity of the antibodies used in the current study are provided in an earlier publication (Chengetanai, Bhagwandin, et al. 2020a) and are not repeated here (see Table 1 for a synopsis of antibody characterization and use in the current study).

2.3 | Analysis

In this study, we provide a qualitative description of the architecture of the somatosensory system in the brain of an African

TABLE 1 | Sources and dilution of antibodies used in the current study.

Antibody	Host	Immunogen	Manufacturer	Catalogue No.	Reference	Dilution	RRID
NeuN	Rabbit	GST-tagged recombinant protein corresponding to mouse NeuN	Merck-Millipore	ABN78C3	Ngwenya et al. 2016	1:500	AB_11204707
ChAT	Goat	Human placental enzyme	Merck-Millipore	AB144P	Laux et al. 2012; Kaiser et al. 2011	1:3000	AB_2079751
TH	Rabbit	Purified tyrosine hydroxylase from rat adrenal	Merck-Millipore	AB151	Piskuric et al. 2011	1:3000	AB_10000323
PV	Rabbit	Rat muscle parvalbumin	Swant	PV28	Celio 1990	1:10,000	AB_10000343
CB	Rabbit	Rat recombinant calbindin D-28k	Swant	CB38a	Celio 1990	1:10,000	AB_10000340
CR	Rabbit	Recombinant human calretinin containing a 6-his tag at the N-terminal	Swant	7699/3H	Schwaller et al. 1997	1:10,000	AB_10000321
vGlut2	Mouse	Recombinant protein from rat vGlut2	Merck-Millipore	MAB5504	Wong et al. 2008; Griffin et al. 2010	1:4000	AB_2187552
SMI-32	Mouse	Non-phosphorylated epitope of neurofilament H from rat hypothalami	Covance	SMI-32R	Sternberger and Sternberger 1983	1:1000	AB_509997

Note: NeuN = neuronal nuclear marker; ChAT = choline acetyltransferase; TH = tyrosine hydroxylase; PV = parvalbumin; CB = calbindin; CR = calretinin; vGlut2 = vesicular glutamate transporter 2; SMI-32 = neurofilament H.

wild dog (LP2). While broadly guided by previous studies in the domestic dog (Singer 1962) and numerous other studies of other mammals (e.g., Kaas 2012; Sawyer 2017; ten Donkelaar et al. 2020), we systematically examined all coronal sections of all stains at low magnification throughout the brain of LP2 to identify regions of interest that correlated with previous reports on the structure of the somatosensory system. For example, when the dorsal column nuclei were identified, we examined the sections in which these nuclei were identified at a range of magnifications to determine precise borders and to note how different nuclei forming this region of the brain were differentiated from each other to develop the description provided. As a second example, the primary somatosensory cortical area (area 3b) was readily delineated due to the intense layer 4 immunostaining with vGlut2. Camera-lucida drawings (see Section 3.7) were made of the right hemisphere, and the border of area 3b was marked. The cortical territories surrounding area 3b were then examined in detail, using all stains, to determine the somatosensory areas surrounding area 3b and delineate them on the camera-lucida drawings. These drawings were aligned with images of the brain to determine the location of these cortical areas on the cortical mantle, and the boundaries were drawn. Our analysis is primarily compared to the atlas of the dog brain provided by Singer (1962), although we employ, as much as is reasonable, the nomenclature provided by Jones (2007) and Paxinos et al. (2009).

3 | Results

The somatosensory and vestibular systems of the African wild dog are composed of a range of nuclear complexes, fiber tracts, and cortical territories. We note that these are very similar to those observed in other carnivore and mammalian species previously described and include, in ascending order, the dorsal column nuclei; the trigeminal sensory nuclear column; the medial lemniscus and trigeminothalamic tracts; the vestibular nuclear complex; portions of the superior and inferior colliculi; the somatosensory nuclei of the dorsal thalamus; and the somatosensory cortex. Here, we provide a systems-level description of these portions of the African wild dog brain. We note here that despite a range of immunohistochemical stains being used, for the sake of brevity, we only report staining patterns that revealed specific features relating to the organization of the somatosensory system.

3.1 | Dorsal Column Nuclei

Within the dorsomedial aspect of the caudal medulla oblongata, the dorsal column nuclei, the nuclei in which the gracile (gr) and cuneate (cu) fasciculi terminate, were observed (Figure 1). The gracile and cuneate fasciculi were rostral extensions of the fiber pathways that formed the dorsal funiculus of the spinal cord, transmitting tactile and proprioceptive information from the body to the dorsal column nuclei. The most medially located dorsal column nucleus was the gracile nucleus (Gr), forming a distinct neuronal cluster dorsal to the rostral opening of the central canal and capped dorsally by the densely myelinated gracile fasciculus (Figure 1). Located laterally adjacent to the gracile nucleus and fasciculus were the cuneate fasciculus and the cuneate nuclear complex, the latter comprising three distinct nuclei, the cuneate nucleus (Cu), the rotundus part of the cuneate nucleus (CuR), and

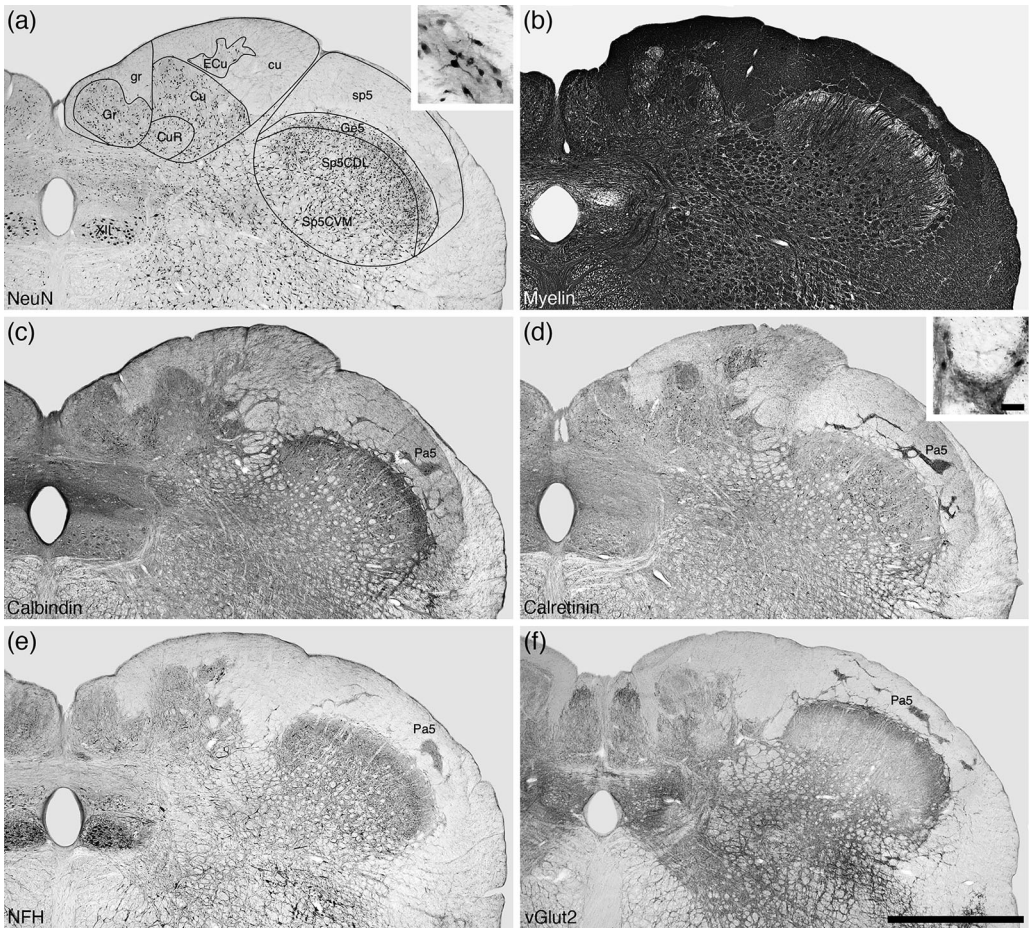

FIGURE 1 | Photomicrographs of coronal sections through the dorsal column and trigeminal nuclear complexes of the African wild dog caudal medulla (at the level of the obex and hypoglossal nucleus—XII) stained for (a) neuronal nuclear marker (NeuN), (b) myelin, (c) calbindin, (d) calretinin, (e) neurofilament H (NFH), and (f) vesicular glutamate transporter 2 (vGlut2). In the dorsal column nuclear complex, we could readily identify the gracile nucleus (Gr) and gracile fasciculus (gr) forming the medial portion of this complex, while the lateral portion was composed of the cuneate nucleus (Cu), the rotundus part of the cuneate nucleus (CuR), the cuneate fasciculus (cu), and the external cuneate nucleus (ECu). In the trigeminal nuclear complex, we could identify the spinal trigeminal tract (sp5), which formed the dorsolateral border of the gelatinous layer of the caudal spinal trigeminal nucleus (Ge5), ventromedial to which was the caudal part of the spinal trigeminal nucleus (Sp5C) that can be subdivided into distinct dorsolateral (Sp5CDL) and ventromedial (Sp5CVM) divisions (see text). The paratrigeminal nucleus (Pa5) was formed of distinct neuronal clusters in the sp5 (b–f) and are shown at higher magnification in the insets of (a) (NeuN) and (d) (calretinin), where, in addition to neurons, a high density of calretinin-immunopositive terminals can be observed in this nucleus. In all images, medial is to the left and dorsal is to the top. Scale bar in (f) = 2 mm and applies to all. Scale bar in inset (d) = 50 μm and applies to both insets.

the external cuneate nucleus (ECu) (Figure 1). The cuneate fasciculus formed a distinct, heavily myelinated dorsal cap, embedded in which were lobulated neuron clusters that formed the ECu. The Cu was the largest of these three divisions, extending from medial to ventrolateral across this nuclear complex, while the CuR occupied the ventromedial half of the nuclear complex (Figure 1). NeuN immunostaining revealed that the Gr, Cu, and CuR have, as judged qualitatively, similar densities of neurons that were of approximately equal size, although slightly smaller in the CuR, while the ECu had a lower neuronal density of slightly larger neurons (Figure 1a). All four dorsal column nuclei exhibited a high density of myelinated fibers, although distinctly less dense than the dorsally adjacent gracile and cuneate fasciculi (Figure 1b). Calbindin- and calretinin-immunopositive neurons were observed at a relatively low density in the Gr, Cu, and CuR, while a high density of calretinin-immunopositive neurons was observed in the ECu (Figure 1c,d). Immunohistochemical staining for neurofilament H revealed a low density of larger dendrites in the Gr, Cr, and CuR, while both soma and dendrites were neurofilament H-immunopositive in the ECu (Figure 1e). Distinct neuropil immunoreactivity for vesicular glutamate transporter 2 was noted in all four nuclei, with the staining intensity being qualitatively strongest in the most dorsal portion of the Gr (Figure 1f). No distinct modular organization of these four dorsal column nuclei was observed with any of the stains used in the current study.

3.2 | The Trigeminal Sensory Nuclear Column

The sensory portion of the trigeminal nerve (s5) of the African wild dog entered the brain through the ventrolateral aspect of the pontine nucleus (Chengetanai, Tenley, et al. 2020). This nerve then pierced the middle cerebellar peduncle and pontine nucleus

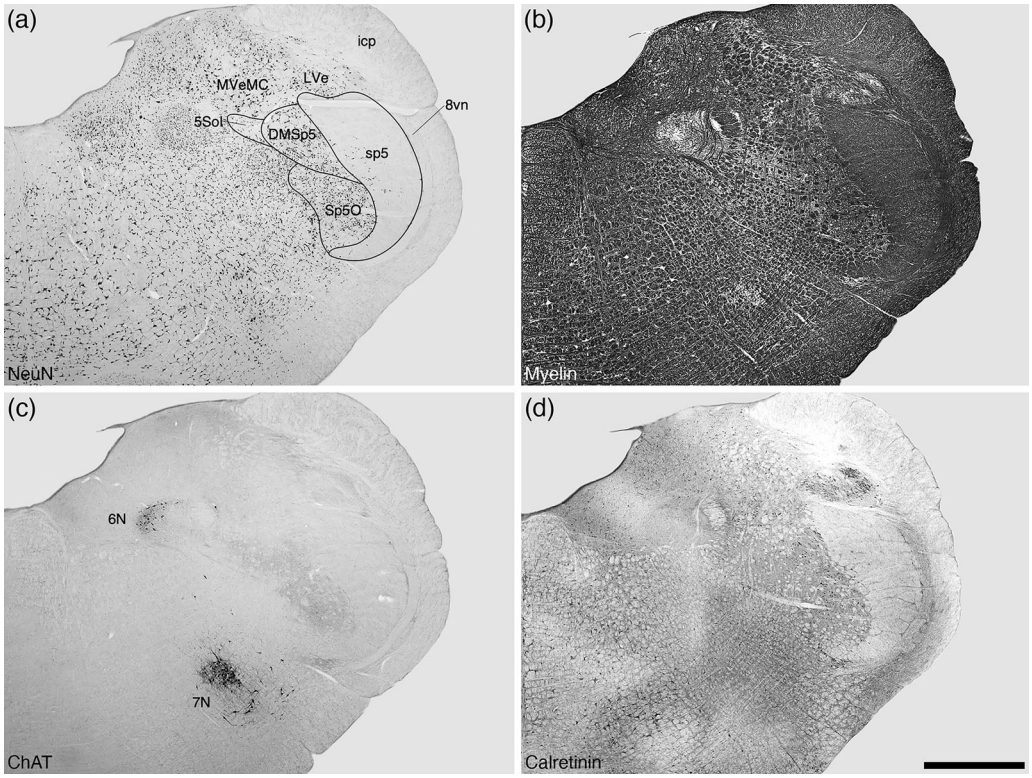

FIGURE 2 | Photomicrographs of coronal sections through the trigeminal nuclear complex of the African wild dog rostral medulla, at the level of the abducens (6N) and facial (7N) cranial nerve nuclei (c) stained for (a) neuronal nuclear marker (NeuN), (b) myelin, (c) choline acetyltransferase (ChAT), and (d) calretinin. The oral part of the spinal trigeminal nucleus (Sp5O), the dorsomedial spinal trigeminal nucleus (DMSp5), and the trigeminal–solitary transition zone (5Sol) are located medial to the spinal trigeminal tract (sp5). At this level of the medulla oblongata, the trigeminal nuclear complex is bordered dorsally by the magnocellular part of the medial vestibular nucleus (mVeMC) and the lateral vestibular nucleus (LVe), laterally and ventrally by the vestibular root of the vestibulocochlear nerve (8vn) and the inferior cerebellar peduncle (icp), and medially by the parvicellular reticular nucleus. In all images, medial is to the left and dorsal is to the top. Scale bar in (d) = 2 mm and applies to all.

in a dorsomedial trajectory to enter the pontine tegmentum, where most of the axons forming this nerve coursed caudally to form the spinal trigeminal tract (sp5). The spinal trigeminal tract was a distinct myelinated pathway, with a curved appearance, on the lateral aspect of the tegmentum of the pons, extending throughout the medulla to the cervical spinal cord, a trajectory and appearance commonly found across mammals (Figures 1–3). The sp5 provided input to a distinct column of nuclei located medially adjacent to this pathway and laterally adjacent to the parvicellular reticular nucleus, this being the trigeminal sensory nuclear column.

The trigeminal sensory nuclear column could be parcellated into several distinct nuclei/part, which, from rostral to caudal, we could readily identify (1) the caudal spinal trigeminal nucleus (Sp5C), with the distinct gelatinous layer of this nucleus (Ge5) and the laterally adjacent paratrigeminal nucleus (Pa5), extended from the nucleus ambiguus to the spinomedullary junction (Figure 1); (2) the dorsomedial spinal trigeminal nucleus (DMSp5) extended from the rostral pole of the facial nerve nucleus to the rostral pole of nucleus ambiguus, and the oral part of spinal trigeminal nucleus (Sp5O) extended from the superior olive to the facial nerve nucleus (Figure 2); and (3) the dorsomedial (Pr5DM) and ventrolateral (Pr5VL) parts of the principal sensory trigeminal nucleus in the caudal pons at the level of the trigeminal motor nucleus (Vmot) (Figure 3). We could not identify dorsal and ventral subdivisions of the DMSp5, the interpolar spinal trigeminal nucleus, or the ectotrigeminal nucleus as reported in the laboratory rat (Paxinos et al. 2009).

In the caudal portion of the medulla oblongata, we identified the relatively large caudal spinal trigeminal nucleus (Sp5C). This nucleus was bordered dorsolaterally by the gelatinous layer of this nucleus (Ge5), with the paratrigeminal nucleus (Pa5) and the spinal trigeminal tract (sp5) found dorsolateral to the Ge5 (Figure 1). Neurons within the Sp5C revealed a distinct dorsolateral-to-ventromedial gradient in density, with the neurons in the dorsolateral aspect of this nucleus having smaller somata than those in the ventromedial aspect of the nucleus (not shown). It is possible, on this basis, to subdivide the Sp5C of the African wild dog into dorsolateral (Sp5CDL) and ventromedial (Sp5CVM) parts. Myelin staining supports this proposed subdivision, with the Sp5CDL exhibiting many distinct myelin fascicles arising from the sp5 investing into and passing through this division to the Sp5CVM. In addition, the Sp5CVM contains several rostrocaudally oriented myelin fascicles not observed in the Sp5CDL (Figure 1b). The density of both calbindin- and calretinin-immunopositive neurons was higher in the Sp5CDL compared to the Sp5CVM (Figure 1c,d). NFH-immunopositive somata were only observed in the Sp5CVM (Figure 1e), while vGlut2 immunostaining was more intense in the Sp5CVM compared to the Sp5CDL (Figure 1f). This series of

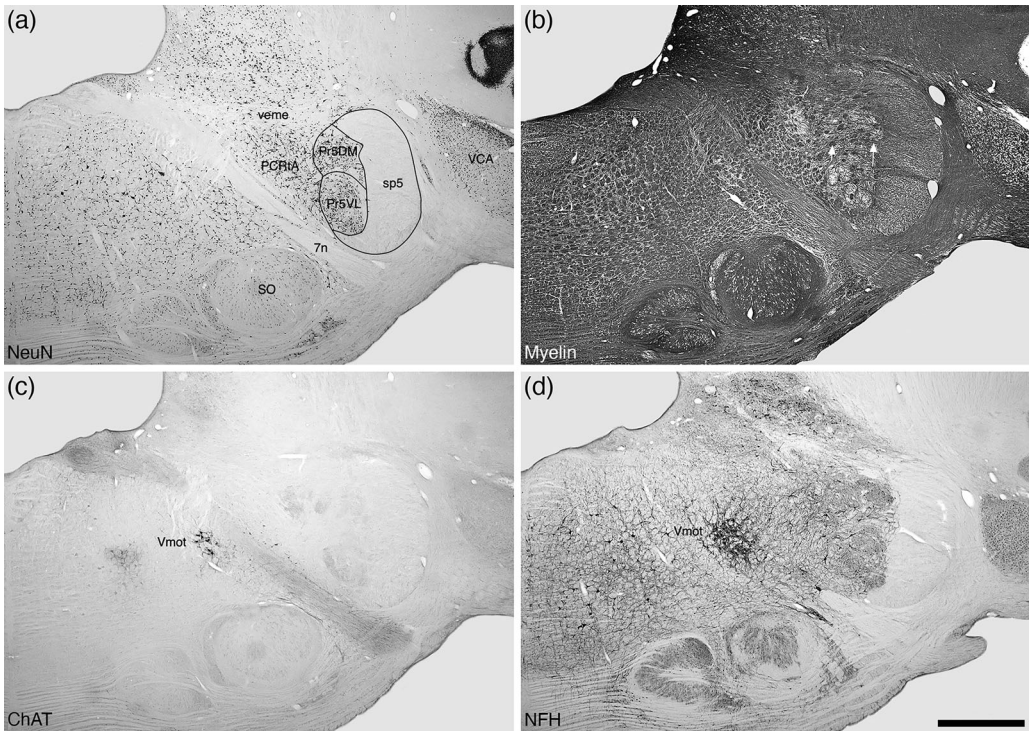

FIGURE 3 | Photomicrographs of coronal sections through the trigeminal nuclear complex of the African wild dog at the level of the caudal pons, where the superior olivary nuclear complex (SO), the anterior part of the ventral cochlear nucleus (VCA), and the caudal pole of the trigeminal motor nucleus (Vmot) were located. These sections were stained for (a) neuronal nuclear marker (NeuN), (b) myelin, (c) choline acetyltransferase (ChAT), and (d) neurofilament H (NFH). At this level of the pons, the spinal trigeminal tract (sp5) forms the lateral border to the dorsomedial (Pr5DM) and the ventrolateral (Pr5VL) parts of the principal sensory trigeminal nucleus. These two nuclear parts are bordered medially by the alpha part of the parvicellular reticular nucleus (PCRtA), ventromedially by the facial nerve (7n), dorsomedially by the vestibulomesencephalic tract (veme), and laterally by the sp5. In (b), the white arrows indicate examples of the rostrocaudally (short arrow) and mediolaterally (long arrow) oriented fibers associated with these nuclei (see text). In all images, medial is to the left and dorsal is to the top. Scale bar in (d) = 2 mm and applies to all.

observations indicates that it would be reasonable to parcellate the Sp5C nucleus into the Sp5CDL and Sp5CVM parts in the African wild dog. Surrounding the dorsolateral edge of the Sp5C, a thin layer of neurons formed the gelatinous layer of the caudal spinal trigeminal nucleus (Ge5). While the Ge5 is not readily distinguished from the Sp5C using cytoarchitectural criteria (Figure 1a), the Ge5 is distinctly myelin sparse and is traversed by the myelin fascicles arising from the sp5 that terminate in the Sp5C (Figure 1b). The Ge5 is marked by intense calbindin-immunopositive neuropil and neurons (Figure 1c) but contains only a few calretinin-immunopositive neurons (Figure 1d). The Ge5 is clearly delineated with vGlut2-immunopositive neuropil staining (Figure 1f). External to the Ge5, lying within the sp5, clusters of neurons, within regions of low myelin density, were revealed with NeuN, calbindin, calretinin, NFH, and vGlut2 immunostaining (Figure 1, also see insets in 1a and 1d). These neuronal clusters were assigned to the paratrigeminal nucleus (Pa5).

In the rostral portion of the medulla oblongata, we identified two distinct trigeminal nuclei—the dorsomedial spinal trigeminal nucleus (DMSp5) and the oral part of the spinal trigeminal nucleus (Sp5O) (Figure 2). The DMSp5 occupied the dorsal half of the trigeminal sensory nuclear column, contained a moderate density of heterogeneously distributed multipolar neurons, some which were observed in the sp5 (Figure 2a), was densely myelinated with a substantive density of rostrocaudally oriented myelinated fascicles (Figure 2b), showed pale neuropil staining for choline acetyltransferase (Figure 2c), and exhibited a low density of calretinin-immunopositive neurons (Figure 2d). Dorsomedial to the DMSp5, a region of small neurons, located ventral to the magnocellular part of the medial vestibular nucleus (MVeMC), corresponded with the trigeminal–solitary transition zone (5Sol) (Figure 2a). The Sp5O occupied the ventral half of the trigeminal sensory nuclear column, and while it contained a similar density of neurons to the DMSp5, these neurons were distributed in a more homogeneous manner throughout the nucleus (Figure 2a). Sp5O exhibited a similar myelin density to that observed in the DMSp5 (Figure 2b). The neuropil staining for choline acetyltransferase in the Sp5O was more intense than observed in the DMSp5, but still faint (Figure 2c), while the presence and distribution of calretinin-immunopositive neurons were similar in both the Sp5O and the DMSp5 (Figure 2d).

In the caudal portion of the pons, the Pr5DM was located immediately dorsal to the Pr5VL, both being bordered laterally by the sp5 and medially by the parvicellular reticular nucleus (PCRtA) and the descending limb of the facial nerve nucleus (Figure 3). Both nuclei were of approximately the same size and contained a moderate neuronal density, with the neurons of the Pr5DM appearing slightly larger than those of the Pr5VL (Figure 3a). The myelin density in both nuclei was high, with

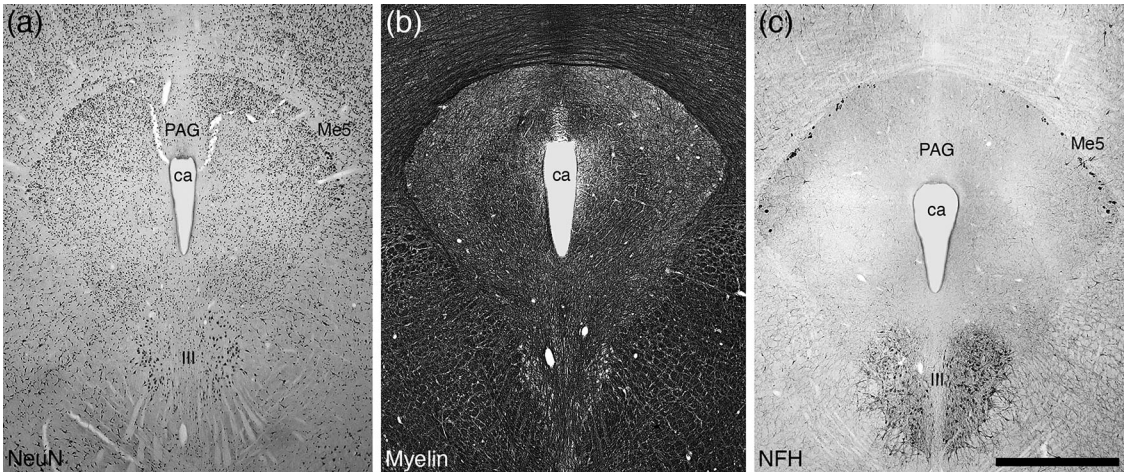

FIGURE 4 | Photomicrographs of coronal sections through the fifth mesencephalic nucleus (Me5) located on the dorsolateral border of the periaqueductal gray matter (PAG) of the African wild dog midbrain stained for (a) neuronal nuclear marker (NeuN), (b) myelin, and (c) neurofilament H (NFH). While stained with NeuN, these Me5 neurons, the only true ganglion cells found within the central nervous system, are clearly labeled with NFH on the dorsolateral border of the PAG. III—oculomotor nucleus; ca—cerebral aqueduct. In all images, dorsal is to the top, with the midline at the center of the image. Scale bar in (c) = 2 mm and applies to all.

distinct mediolaterally oriented fiber bundles arising from the sp5, presumably to innervate these nuclei, and distinct rostrocaudally oriented myelin fascicles throughout the nuclei that likely aggregate to form the trigeminothalamic tract (Figure 3b). In both nuclei, a distinct—although not intense—neuropil staining for choline acetyltransferase was observed (Figure 3c), while immunostaining for neurofilament H revealed several larger multipolar neurons in both nuclei (Figure 3d).

A small portion of the s5, the tract of the fifth mesencephalic nucleus (Vmestr), branched rostrally within the pontine tegmentum and ran adjacent to the ventrolateral aspect of the periventricular and then periaqueductal gray matter to supply sensory input to the ganglionic neurons that formed the fifth mesencephalic nucleus (Me5). The neurons forming the Me5 were located on the dorsolateral aspect of the periaqueductal gray matter, at the level of the oculomotor nucleus (Figure 4). The neurons of the Me5 had large, round somata and were the only ganglionic neurons observed within the central nervous system of the African wild dog. Me5 neurons were clearly revealed with Nissl staining, NeuN immunostaining (Figure 4a), and neurofilament H immunostaining (Figure 4c).

3.3 | Medial Lemniscus and Trigeminothalamic Tracts

The ascending internal arcuate fibers, which arise from the neurons of the gracile and cuneate nuclei, were observed to decussate in the rostral medulla oblongata (not shown) and form the distinct medial lemniscus. The medial lemniscus was located dorsal to the pyramidal tract in the medulla oblongata. At the more rostral pontine level, the medial lemniscus was located in the ventrolateral aspect of the pons immediately dorsal to the pontine nucleus (Figure 5). In the midbrain, the medial lemniscus was observed in a position lateral to the red nucleus, from which it was observed to invest into the ventral posterior nuclear complex of the dorsal thalamus (see Section 3.6). The ascending fibers arising from the rostrocaudally elongated trigeminal sensory nuclear column were observed to decussate and form the trigeminothalamic tract found immediately dorsal to the medial lemniscus (Figure 5). The trigeminothalamic tract followed the same trajectory as the medial lemniscus to invest into the ventral posterior nuclear complex of the dorsal thalamus (see Section 3.6). Our preparations did not allow us to readily identify the anterolateral system (composed of the spinothalamic, spinoreticular, and spinomesencephalic tracts) (e.g., Willis and Westlund 1997), although they are likely to be present in the African wild dog.

3.4 | The Vestibular Nuclear Complex

The vestibular nuclear complex was identified in the dorsolateral aspect of the rostral medulla oblongata, bordered dorsomedially by the white matter and nuclei of the cerebellum, dorsolaterally by the inferior cerebellar peduncle, medially by the genu of the facial nerve and the fourth ventricle, ventrally by the trigeminal sensory nuclei, and laterally by the vestibular part of the eighth nerve (8vn) from which this nuclear complex receives incoming sensory information (Figure 6). Within this nuclear complex, we could readily identify six distinct nuclei, including the superior (SuVe), parvocellular part of the medial (mVePC), magnocellular part of the medial (mVeMC), lateral (LVe), and vestibulocerebellar (VeCb) vestibular nuclei (Figure 6) and the spinal vestibular nucleus (SpVe) (not depicted). The location of this nuclear complex, as well as the relative internal organization of the nuclei forming this complex, is like that observed in more frequently studied mammals (e.g., Paxinos et al. 2009). Immunohistochemical staining for neurofilament H revealed the large neurons forming the LVe, as well as the slightly smaller neurons of the mVeMc and VeCb (Figure 6c). While many neurons within this nuclear complex were moderately intensely immunostained for parvalbumin, we observed a striking density of parvalbumin-immunopositive axonal terminals forming pericellular baskets that enveloped the large neurons of the LVe (Figure 6d).

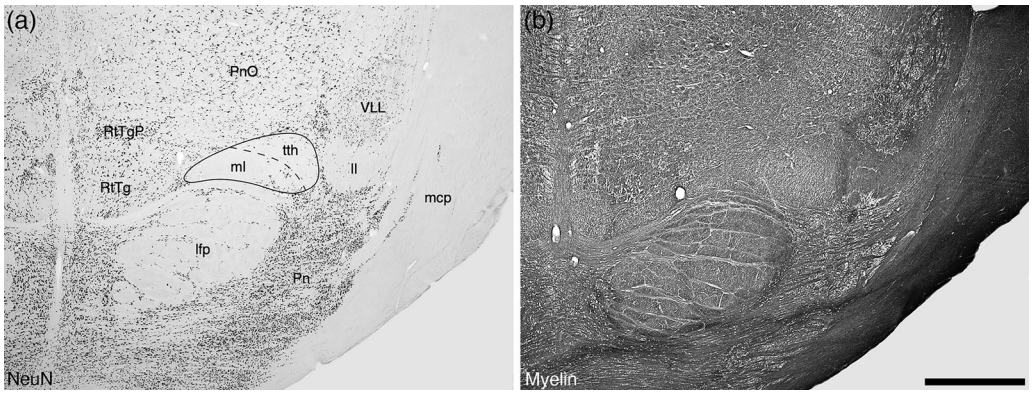

FIGURE 5 | Photomicrographs of coronal sections through the medial lemniscus (ml) and the trigeminothalamic tract (tth) of the African wild dog at the level of the pontine nucleus (Pn) stained for (a) neuronal nuclear marker (NeuN) and (b) myelin. Note that the demarcation of the ml and tth is not absolutely clear (marked by a dashed line). The ml/tth are located in a position consistent with what is reported in the rat (Paxinos et al. 2009), being bordered ventrally by the longitudinal fasciculus of the pons (lfp) and Pn, medially by the pericentral part (RtTgP) of the reticulotegmental nucleus of the pons (RtTg), dorsally by the oral part of the pontine reticular nucleus (PnO), and laterally by the lateral lemniscus (ll), the ventral nucleus of the lateral lemniscus (VLL), and the middle cerebellar peduncle (mcp). In both images, medial is to the left and dorsal is to the top. Scale bar in (b) = 2 mm and applies to both images.

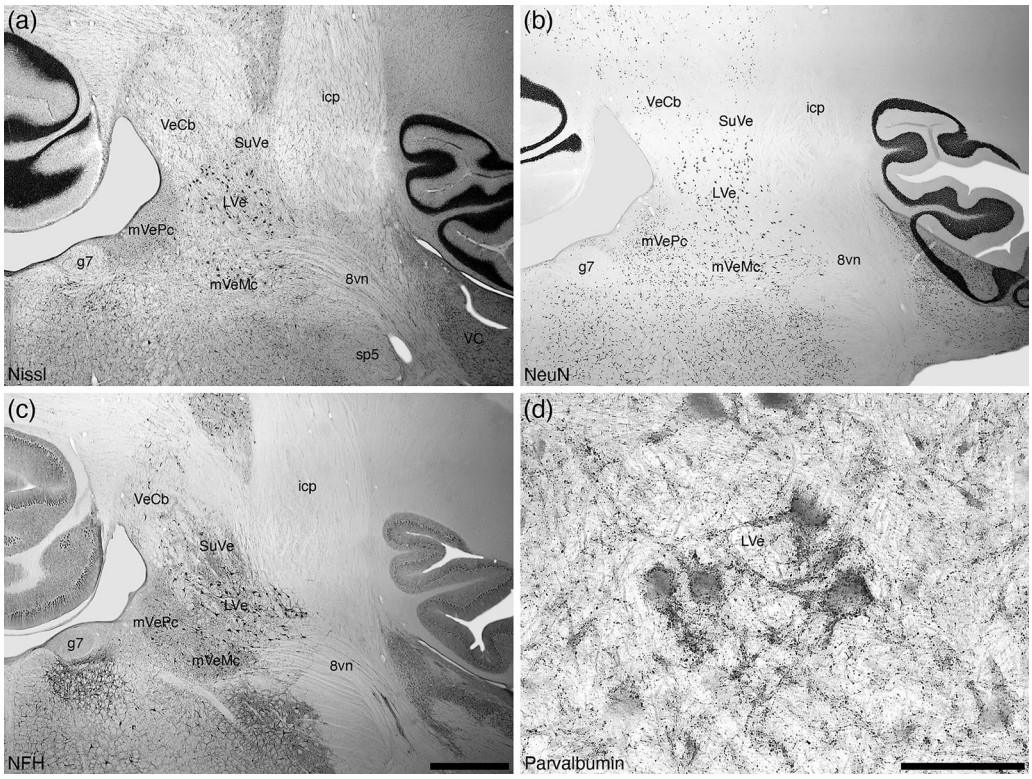

FIGURE 6 | Photomicrographs of coronal sections through the vestibular nuclear complex of the African wild dog stained for (a) Nissl, (b) neuronal nuclear marker (NeuN), and (c) neurofilament H (NFH), with a higher magnification image of (d) parvalbumin. Several nuclei of the vestibular nuclear complex were readily observed in the African wild dog brain including the lateral vestibular nucleus (LVe), the magnocellular part of the medial vestibular nucleus (mVeMc), the parvocellular part of the medial vestibular nucleus (mVePc), the superior vestibular nucleus (SuVe), and the vestibulocerebellar nucleus (VeCb), innervated by the vestibular part of the eighth nerve (8vn) (a–c). (d) The somata of the large neurons of the LVe are densely innervated by parvalbumin-immunopositive terminals. In all images, medial is to the left and dorsal is to the top. Scale bar in (c) = 2 mm and applies to (a–c). Scale bar in (d) = 200 μm and applies to (d). g7—genu of the facial nerve; icp—inferior cerebellar peduncle; sp5—spinal trigeminal tract; VC—ventral cochlear nucleus.

3.5 | Inferior and Superior Colliculi

The external cortical nucleus of the inferior colliculus is known to receive ascending somatosensory input from the dorsal column nuclei (Schroder and Jane 1976). The location and neurochemistry of this nuclear subdivision of the inferior colliculus have been described in detail previously (Chengetanai, Bhagwandin, et al. 2020b) and are not described further herein. The intermediate and deep layers of the superior colliculus receive input from several somatosensory nuclei and cortical areas (Liu et al. 2022). The location and neurochemistry of the layers of the superior colliculus have been described in detail previously (Chengetanai, Bhagwandin, et al. 2020c) and are not described further herein.

3.6 | Somatosensory Nuclei of the Dorsal Thalamus

Most of the somatosensory-related region of the dorsal thalamus is occupied by the four nuclei forming the ventral posterior nuclear group but also includes the medial division of the posterior nucleus (Pom) (Jones 2007). The ventral posterior nuclear group is organized into the ventral posterior medial nucleus (VPM, associated with trigeminal inputs), the ventral posterior lateral nucleus (VPL, associated with spinal inputs), the basal ventral medial nucleus (VMb, associated with taste and other visceral afferents), and the ventral posterior inferior nucleus (VPI, where the medial lemniscus invests and is associated with Pacinian corpuscle, or vibration, input) (Jones 2007). This often-observed arrangement of the mammalian somatosensory thalamic nuclei (Jones 2007) was evident in the dorsal thalamus of the African wild dog (Figure 7).

The borders of the ventral posterior nuclear group were readily distinguished with both cytoarchitecture (Figure 7a) and myeloarchitecture (Figure 7b), as well as with parvalbumin (Figure 7c) and vesicular glutamate transporter 2 (Figure 7d) immunostaining. The VPM occupied the medial portion of the nuclear group, while the VPL occupied the lateral portion. The density of neurons located in VPM and VPL was quite similar, as was the density of myelinated fibers. A relatively homogeneous neuropil immunostaining for parvalbumin was identified in both VPM and VPL. In contrast, the vesicular glutamate transporter 2 immunostaining was relatively patchy in appearance, with the most medial aspect of the VPM (potentially correlating to the orofacial trigeminal representation) revealing the most distinct heterogeneity (Figure 7d). The VPI was located at the ventral middle portion of the nuclear group, located at the ventral-most border of the shared VPM/VPL border. VPI exhibited a slightly lower neuronal density than VPM/VPL but had similar intensities of staining for myelin and parvalbumin; however, the VPI had very-low-intensity vesicular glutamate transporter 2 immunostaining (Figure 7). The VMb was located on the most ventromedial aspect of the ventral posterior nuclear group. While showing a similar neuronal density and parvalbumin neuropil staining intensity to the VPM and VPL, the density of myelin was much lower, and there was a very low-intensity vesicular glutamate transporter 2 immunostaining (Figure 7).

The medial division of the posterior nucleus (Pom) was observed as a thin sheet of neurons lying dorsal to the VPM and VPL, between these nuclei and the vision-associated lateral posterior nucleus (Figure 7; see also figure 2 in Chengetanai, Bhagwandin, et al. [2020c]). The density of neurons was slightly lower than observed in the VPM and VPL, while the myelin density and parvalbumin neuropil staining intensity were comparable to these nuclei. A very-low-intensity vesicular glutamate transporter 2 immunostaining was observed in Pom (Figure 7d).

3.7 | Somatosensory Areas of the Cerebral Cortex

Our cyto-, myelo-, and chemoarchitectural analysis of the cerebral cortex in the African wild dog revealed the presence of five distinct cortical areas, three of which were located medially on the cortical mantle, while two were located laterally adjacent to these areas. The somatosensory cortical areas were located caudal to the cruciate sulcus, occupying the posterior sigmoid gyrus, post-cruciate sulcus, posterior cruciate gyrus, coronal gyrus, coronal sulcus, anterior suprasylvian gyrus, and anterior suprasylvian sulcus (Figures 8 and 9). All five cortical areas were composed of six cortical layers, although the distinctiveness of the outer and inner borders of layer 4 varied between areas. The three distinct cortical areas found on the medial aspect of the cortical mantle included, from rostral to caudal, area 3a (a proprioceptive area located between the primary motor and somatosensory cortex), area SI (also called 3b, or the primary somatosensory cortical area), and area SIII (the third somatosensory cortical area, located immediately caudal to area 3b and rostral to the posterior parietal cortical region; Chengetanai, Bhagwandin, et al. 2020c). In the cortex lateral to these three cortical areas, we were able to define cortical area Pv (the parietal–ventral somatosensory cortical area), caudal to which was area SII (the second somatosensory cortical area).

3.7.1 | Area 3a

While neurons were observed in all cortical layers, layer 1 was relatively neuron sparse, while layer 2 exhibited the highest neuronal density. Layers 2 and 4 were composed of granule-shaped neurons, layers 3 and 5 exhibited pyramidal-shaped neurons, while a range of somal shapes were observed in layer 6. Layer 5 exhibited a lower density of neurons compared to cortical layers 2, 3, 4, and 6 (Figure 10a,c). A moderate to high density of myelinated axons was observed in all cortical layers, with the lowest density being observed in layer 2. All cortical layers exhibited horizontally oriented myelinated axons, with a higher density of these axons in layers 4, 5, and 6. Radially oriented myelinated axon fascicles were observed to enter through layer 6, traversing superficially, before ending in the inner half of layer 3 (Figure 10b).

No parvalbumin-immunopositive neurons were observed in area 3a (a characteristic that distinguishes this cortical area from all surrounding areas), although distinct axonal terminal staining was observed in layers 2–6, with a slight increase in density in layer 5. Occasional pericellular baskets of parvalbumin-immunopositive axon terminals were observed surrounding the larger pyramidal neurons in inner layer 3 and layer 5 (Figure 10d). A low density of calbindin-immunopositive neurons was observed in layers 2 and outer layer 3, with a low

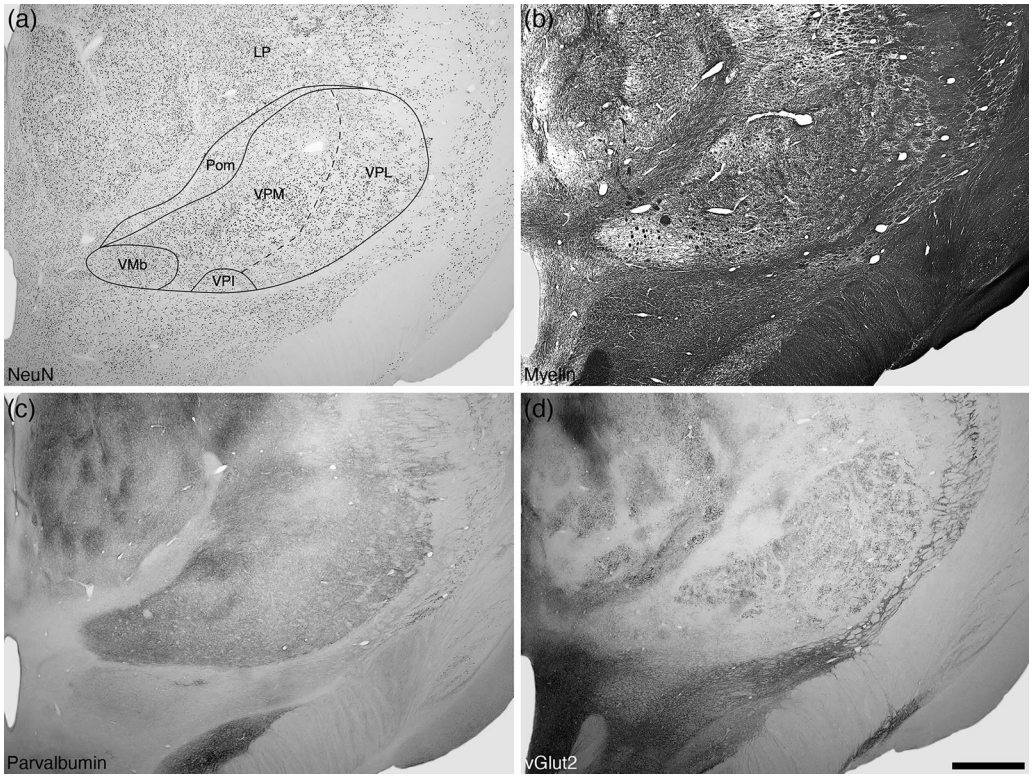

FIGURE 7 | Photomicrographs of coronal sections through the ventral posterior nuclear group of the African wild dog dorsal thalamus stained for (a) neuronal nuclear marker (NeuN), (b) myelin, (c) parvalbumin, and (d) vesicular glutamate transporter 2 (vGlut2). The ventral posterior nuclear group is located in the ventrolateral aspect of the dorsal thalamus and receives axons from the medial lemniscus, trigeminothalamic tract, spinothalamic tract, and central tegmental tract (see Figure 5). Several distinct nuclei were observable, including the ventral posterior medial (VPM), ventral posterior lateral (VPL), ventral posterior inferior (VPI), and basal ventral medial (VMb) nuclei. In addition, the medial posterior nucleus (Pom) processes somatic sensory information. In all images, medial is to the left and dorsal is to the top. Scale bar in (d) = 2 mm and applies to all. LP—lateral posterior nucleus.

density of axonal terminals labeled throughout the cortical layers (Figure 10e). A low density of calretinin-immunopositive neurons was observed in layer 2 and the outer portion of layer 3. These calretinin-immunopositive neurons exhibited distinctly labeled apical dendrites extending into layer 1 (Figure 10f). A low density of NFH-immunopositive pyramidal neurons was observed in inner layer 3, with a moderate to low density of apical dendrites being observed in other cortical layers (Figure 10g). vGlut2-immunopositive axonal terminals were observed in all cortical layers, with layers 4, inner layer 3, and layer 6 showing the highest relative densities (Figure 10h).

3.7.2 | Area 3b (Primary Somatosensory Cortex, SI)

Layer 1 was relatively neuron sparse, while layer 2 exhibited the highest neuronal density. Layer 2 and the cytoarchitecturally distinct layer 4 were composed of granule-shaped neurons, layers 3 and 5 exhibited pyramidal-shaped neurons, while a range of somal shapes was observed in layer 6 (Figure 10i,k). A moderate to high density of myelinated axons was observed in all cortical layers, with the lowest density being observed in layer 2. All cortical layers exhibited horizontally oriented myelinated axons, with a higher density of these axons in the deeper layers. Loosely aggregated radially oriented myelinated axon fascicles were observed to enter through layer 6, traversing superficially, before ending in layer 4 (Figure 10j).

A low density of parvalbumin-immunopositive neurons was observed in layers 2–6, with distinct axonal terminal staining also observed in these layers, showing an increase in density in layer 4 (Figure 10l). A low density of calbindin-immunopositive neurons was observed in layer 2, outer layer 3, layer 5, and layer 6, with a low density of axonal terminals labeled throughout the cortical layers, although this density is slightly higher in layers 1 and 2 (Figure 10m). A low density of calretinin-immunopositive neurons was observed in layer 2 and the outer portion of layer 3, with the occasional neuron being observed in layer 5. These calretinin-immunopositive neurons exhibited distinctly labeled apical dendrites extending into layer 1 (Figure 10n). A low density of NFH-immunopositive pyramidal neurons was observed in outer layer 5, with a moderate to low density of apical dendrites being observed in layers 3–6 (Figure 10o). vGlut2-immunopositive axonal terminals were observed in all cortical layers, with layer 4 and inner layer 3 showing a distinct high density and layer 6 showing a moderate density (Figure 10p).

3.7.3 | Area SIII (The Third Somatosensory Cortical Area)

Layer 1 was neuron sparse, while layers 2, 3, and 6 exhibited higher neuronal densities. Layer 2 and the moderately cytoarchitecturally distinct layer 4 were composed of granule-shaped neurons, layers 3 and 5 exhibited pyramidal-shaped neurons, while

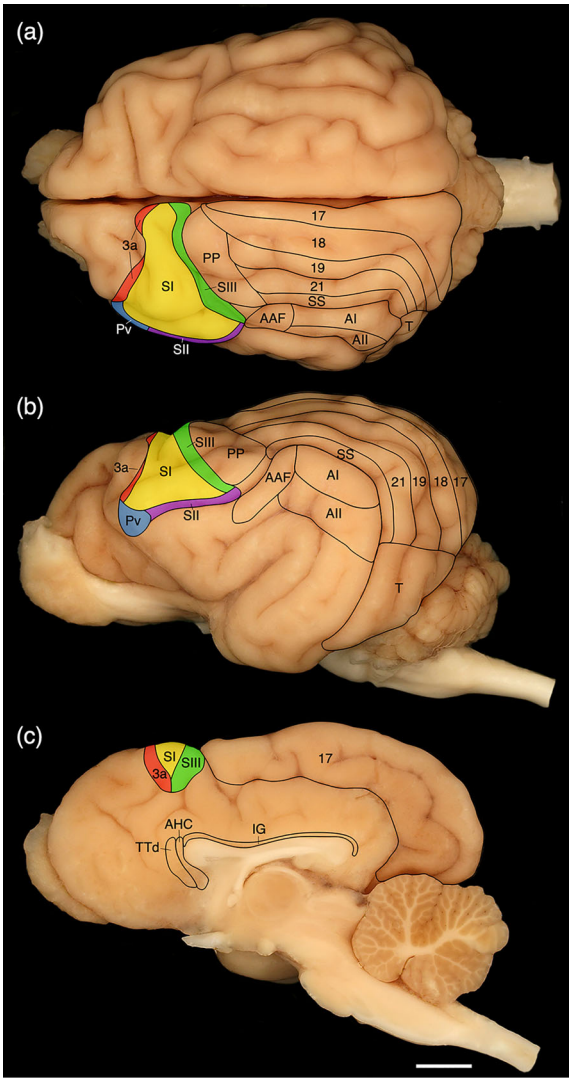

FIGURE 8 | (a) Dorsal, (b) lateral, and (c) midsagittal views of the African wild dog brain showing the approximate location of the somatosensory cortical areas determined with architectural and immunohistochemical stains in the current study (see Figure 10). Within the somatosensory cortex of the African wild dog, we identified five areas, organized into medial (areas 3a [red shading], SI [the primary somatosensory area, yellow shading], and SIII [the third somatosensory area, green shading]) and lateral (Pv [parietal ventral somatosensory area, blue shading] and SII [second somatosensory area, purple shading]) areas. These are placed in relation to cortical areas involved in olfaction (Chengetanai, Bhagwandin, et al. 2020a), audition (Chengetanai, Bhagwandin, et al. 2020b), and vision (Chengetanai, Bhagwandin, et al. 2020b). Scale bar in (c) = 1 cm and applies to all. 17, 18, 19, and 21—occipital visual areas; AAF—anterior auditory field; AI—primary auditory cortex; AII—secondary auditory cortex; AHC—anterior hippocampal continuation; IG—indusium griseum; PP—posterior parietal cortical areas; SS—suprasylvian visual areas; T—temporal visual region; TTd—dorsal taenia tecta.

a range of somal shapes were observed in layer 6 (Figure 11a,c). A moderate to high density of myelinated axons was observed in all cortical layers, with the lowest density in layer 2. All layers exhibited horizontally oriented myelinated axons, with higher axonal densities in the deeper layers. Radially oriented myelinated axon fascicles were observed to enter through layer 6, traversing superficially, before ending in layer 4 (Figure 11b).

A low density of parvalbumin-immunopositive neurons was observed in layer 3, with distinct axonal terminal staining observed in layers 2–6 (Figure 11d). A moderate density of calbindin-immunopositive neurons was observed in layer 2, with occasional neurons observed in layers 3, 5, and 6. A low density of calbindin-immunopositive axonal terminals was observed throughout the cortical layers (Figure 11e). A low to moderate density of calretinin-immunopositive neurons was observed in layer 2, with the occasional neuron being observed in layers 3 and 5. These calretinin-immunopositive neurons exhibited distinctly labeled apical dendrites extending into layer 1 (Figure 11f). A low density of NFH-immunopositive pyramidal neurons was observed in inner layer 3, with a moderate to low density of apical dendrites being observed in layers 2–6 (Figure 11g). vGlut2-immunopositive axonal terminals were observed in all cortical layers, with layer 4 and inner layer 3 showing a distinct moderate density of axonal terminals and layer 6 showing a low to moderate density (Figure 11h).

3.7.4 | Area SII (The Second Somatosensory Cortical Area)

As with the other cortical areas, layer 1 was neuron sparse, while layers 2 and 5 exhibited lower neuronal densities than layers 3, 4, and 6. Layer 2 and the weakly cytoarchitecturally distinct layer 4 were composed of granule-shaped neurons, layers 3 and 5 exhibited pyramidal-shaped neurons, while a range of somal shapes were observed in layer 6 (Figure 12a,c). A moderate to high density of myelinated axons was observed in all cortical layers, with the lowest density in layer 2. All layers exhibited horizontally oriented myelinated axons, with loosely aggregated, radially oriented, myelinated axon fascicles traversing from layer 6 through to layer 2 (Figure 12b).

A low density of parvalbumin-immunopositive neurons was observed in layers 2 and 3, with axonal terminal staining observed in layers 2–6 (Figure 12d). A moderate density of calbindin-immunopositive neurons was observed in layers 2 and 3, with a low density of calbindin-immunopositive axonal terminals observed throughout the cortical layers (Figure 12e). A low to moderate density of calretinin-immunopositive neurons was observed in layers 2 and 3, with the occasional neuron being observed in layer 4 (Figure 12f). A low density of NFH-immunopositive pyramidal neurons was observed in inner layer 3, with a moderate to low density of apical dendrites being observed in layers 3–6 (Figure 12g). vGlut2-immunopositive axonal terminals were observed in all cortical layers, with layer 4 and inner layer 3 showing a distinctly higher density of axonal terminals than the other cortical layers (Figure 12h).

3.7.5 | Area Pv (The Parietal Ventral Somatosensory Cortical Area)

As with the other cortical areas, layer 1 was neuron sparse, while layers 2 and 5 exhibited lower neuronal densities than layers 3,

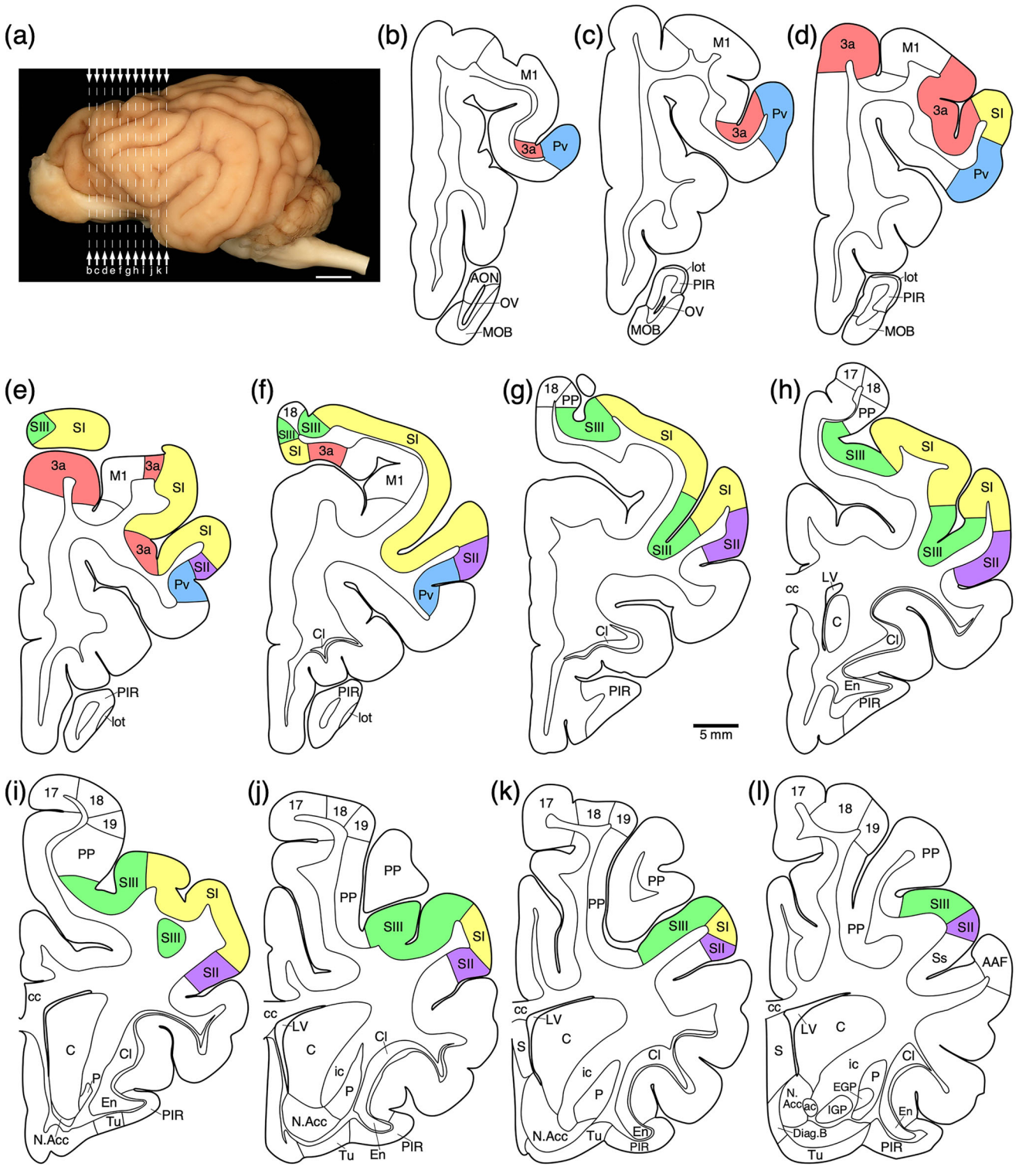

FIGURE 9 | Diagrammatic reconstructions of coronal sections through the African wild dog brain delineating the identified somatosensory cortical areas and certain other subcortical structures. In all diagrams, dorsal is to the top and medial is to the left. Image (a) shows a lateral view of the African wild dog brain with the approximate level of the reconstructed sections. Image (b) represents the most rostral section drawn, while image (l) represents the most caudal section. Each diagram is approximately 2000 μm apart. The various cortical areas are represented with differing colors. 17, 18, and 19—occipital visual area; 3a—proprioceptive somatosensory cortical area; AAF—anterior auditory field; ac—anterior commissure; AON—anterior olfactory nucleus; C—caudate nucleus; cc—corpus callosum; Cl—claustrum; Diag.B—diagonal band of Broca; EGP—external globus pallidus; En—endopiriform nucleus; ic—internal capsule; IGP—internal globus pallidus; lot—lateral olfactory tract; LV—lateral ventricle; M1—primary motor cortical area; MOB—main olfactory bulb; N.Acc—nucleus accumbens; OV—olfactory ventricle; P—putamen; PIR—piriform cortex; PP—posterior parietal visual region; Pv—parietal–ventral somatosensory cortical area; S—septal nuclear complex; SI—primary somatosensory cortical area; SII—second somatosensory cortical area; SIII—third somatosensory cortical area; Ss—suprasylvian visual region; Tu—olfactory tubercle.

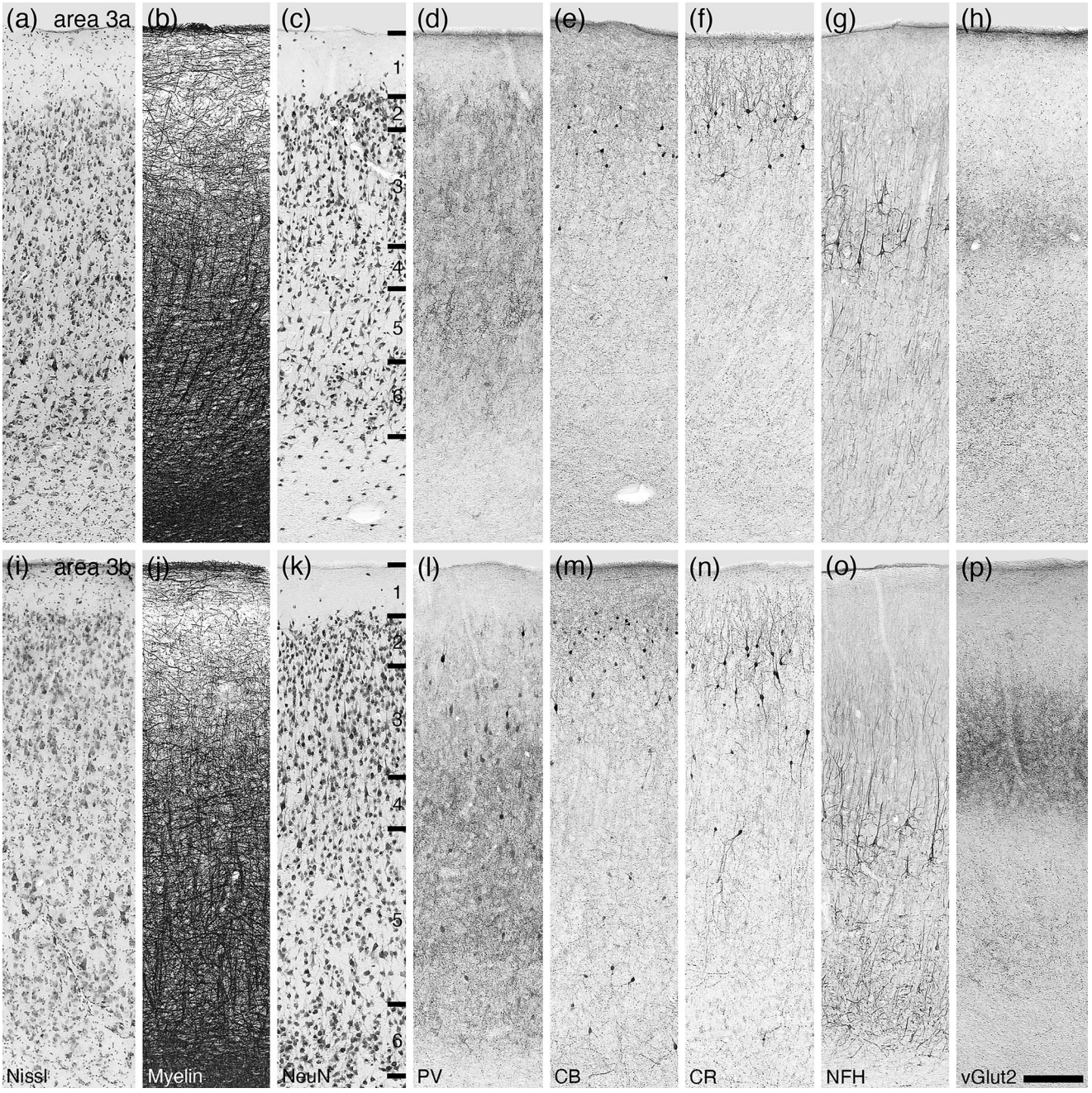

FIGURE 10 | Photomicrographs of sections stained for Nissl (a, i), myelin (b, j), neuronal nuclear marker (NeuN) (c, k), parvalbumin (PV) (d, l), calbindin (CB) (e, m), calretinin (CR) (f, n), neurofilament H (NFH) (g, o), and vesicular glutamate transporter 2 (vGlut2) (h, p) in area 3a (a–h) and area 3b (or primary somatosensory cortex, SI) (i–p) of the African wild dog. In all images, the pial surface is at the top of the image. Layer demarcations are provided in (c) for each cortical area. Scale bar in (p) = 250 μm and applies to all.

4, and 6. Layer 2 and the weak to moderately cytoarchitecturally distinct layer 4 were composed of granule-shaped neurons, layers 3 and 5 exhibited pyramidal-shaped neurons, while a range of somal shapes were observed in layer 6 (Figure 12i,k). A moderate to high density of myelinated axons was observed in all cortical layers, with the lowest densities in layer 2 and outer layer 3. All layers exhibited horizontally oriented myelinated axons, with loosely aggregated, radially oriented, myelinated axon fascicles traversing from layer 6 through to layer 4 (Figure 12j).

A low density of parvalbumin-immunopositive neurons was observed in layers 2 and 3, with axonal terminal staining observed in layers 2–6 (Figure 12l). A moderate density of calbindin-immunopositive neurons was observed in layer 2 and outer layer 3, with occasional neurons in layers 5 and 6 (Figure 12m). A low to moderate density of calretinin-immunopositive neurons was observed in layers 2 and 3, with the occasional neuron being observed in layers 4 and 5 (Figure 12n). A low density of NFH-immunopositive pyramidal neurons was observed in inner layer 3, with a moderate to low density of apical dendrites being observed in layers 2–6 (Figure 12o). vGlut2-immunopositive

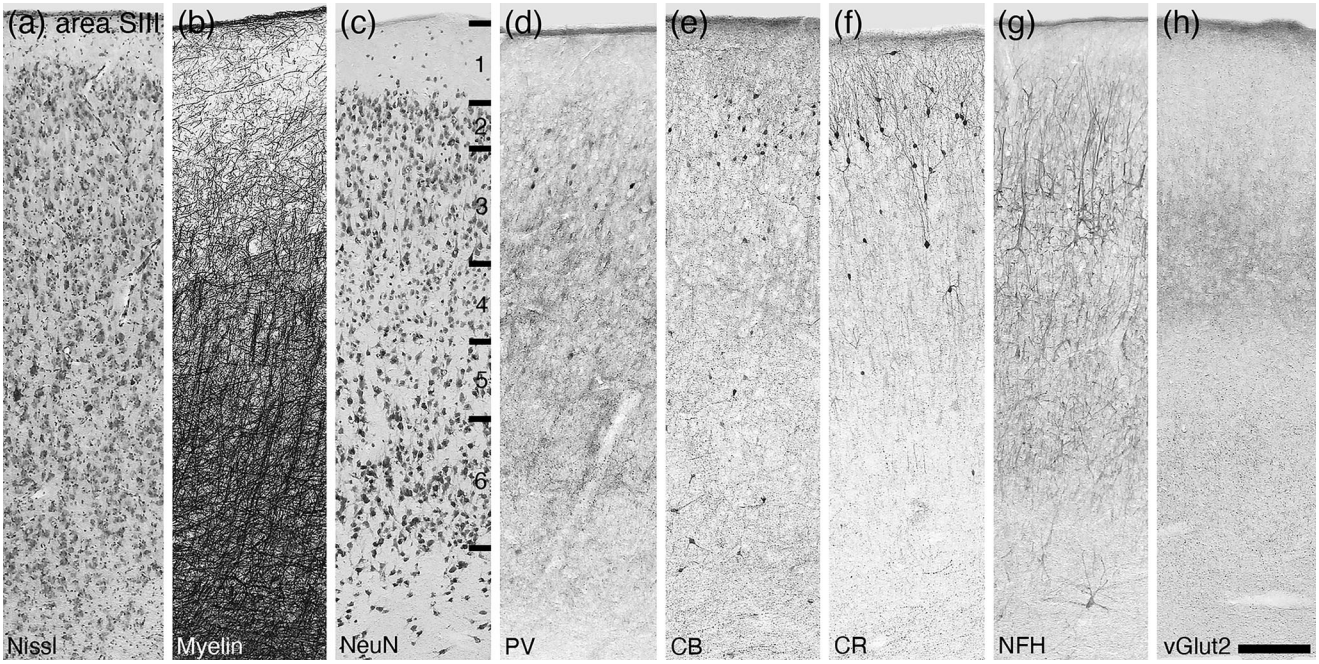

FIGURE 11 | Photomicrographs of sections stained for Nissl (a), myelin (b), neuronal nuclear marker (NeuN) (c), parvalbumin (PV) (d), calbindin (CB) (e), calretinin (CR) (f), neurofilament H (NFH) (g), and vesicular glutamate transporter 2 (vGlut2) (h) in area SIII (the third somatosensory area) of the African wild dog. In all images, the pial surface is at the top of the image. Layer demarcations are provided in (c). Scale bar in (h) = 250 μm and applies to all.

axonal terminals were observed in all cortical layers, with layer 4 and inner layer 3 showing a distinctly higher density of axonal terminals than the other cortical layers (Figure 12p).

4 | Discussion

The current study provides a qualitative systems-level analysis of the somatosensory and vestibular systems in the brain of the African wild dog. This study completes our examination of the major sensory systems in the African wild dog brain, which include the olfactory (Chengetanai, Bhagwandin, et al. 2020a), auditory (Chengetanai, Bhagwandin, et al. 2020b), and visual (Chengetanai, Bhagwandin, et al. 2020c) systems. Our investigations indicate, at the systems level of analysis, that no overt specializations of the sensory systems can be observed, particularly in comparison to those reported in the domestic dog (e.g., Singer 1962). Our central motivation for this series of studies is to determine whether the complex social behavior of African wild dogs (Creel and Creel 2002) correlates with any specific specializations within the brain. We can now conclude that, in terms of sensory systems at the level of analysis undertaken, there appear to be no specific senses that are overtly specialized for the direct support of social behaviors in the African wild dog.

4.1 | Comparison of the Somatosensory System of the African Wild Dog

In the current study, we did not find any features of the somatosensory system within the brain of the African wild dog that were clearly different from those reported in the domestic dog (Singer 1962). Indeed, the organization of the African wild dog brain is generally very much like that typically observed across mammals (e.g., Kaas 2012; Sawyer 2017; ten Donkelaar et al. 2020). The location and appearance of the dorsal column nuclei, the trigeminal sensory column, and the colliculi in the brainstem of the African wild dog are very similar to those observed in the domestic dog (Singer 1962), in other carnivores (e.g., Sawyer et al. 2016; Sawyer and Sarko 2017; Sawyer 2017), and in other mammals (e.g., Paxinos et al. 2009; Maseko et al. 2013; Imam et al. 2019). The organization of the somatosensory nuclear complex of the dorsal thalamus of the African wild dog is like that observed in the domestic dog (Singer 1962) and most other mammals (e.g., Manger et al. 2001; Jones 2007; Paxinos et al. 2009; Maseko et al. 2013; Sawyer et al. 2016; Imam et al. 2019). This includes the number of nuclei comprising the ventral posterior nuclear group and the medial posterior nucleus, as well as their interrelations with each other and with other nuclei comprising the dorsal thalamus.

The location of area 3b (SI) and SII in the African wild dog—based on the presence of distinct and intense vesicular glutamate transporter 2 immunostaining in layer 4 or area 3b, and the relationship of these two cortical regions to the pattern of sulci and gyri and to the visual and auditory cortex—is similar to that observed in studies of the domestic dog (e.g., Norrsell 1978; Guran et al. 2024) and the domestic cat (e.g., Clemo and Stein 1983; Schwark et al. 1992; Clemo and Meredith 2004). Indeed, the five somatosensory cortical areas identified with the range of stains used in the current study of the African wild dog are like those previously described in the domestic dog (Norrsell 1978; Guran et al. 2024), domestic cat (Clemo and Stein 1983; Schwark et al. 1992; Clemo and Meredith 2004), and domestic ferret (Foxworthy and Meredith 2011). This indicates that in the Carnivora, the somatosensory cortex is likely to be composed of the same

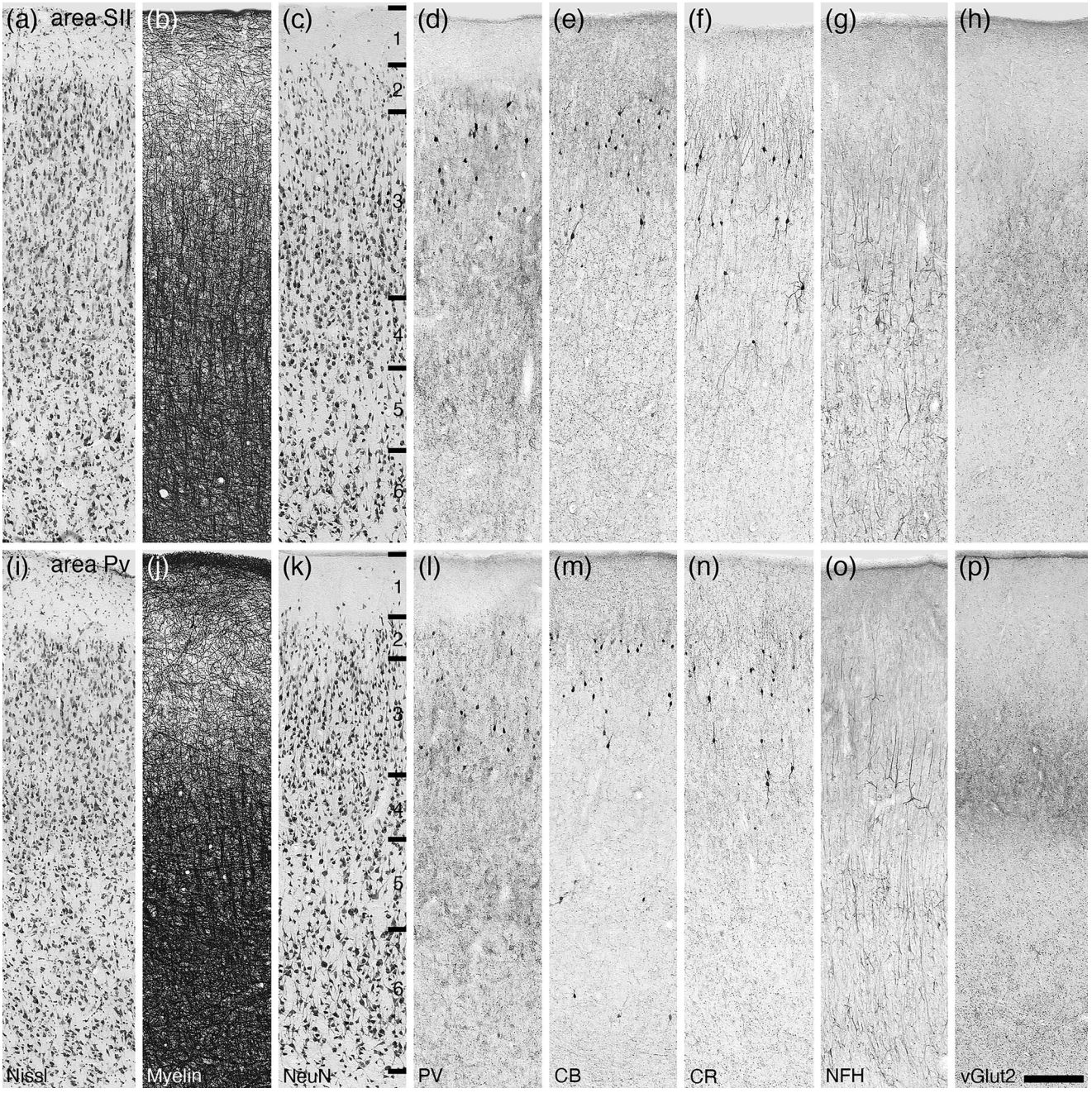

FIGURE 12 | Photomicrographs of sections stained for Nissl (a, i), myelin (b, j), neuronal nuclear marker (NeuN) (c, k), parvalbumin (PV) (d, l), calbindin (CB) (e, m), calretinin (CR) (f, n), neurofilament H (NFH) (g, o), and vesicular glutamate transporter 2 (vGlut2) (h, p) in area SII (the second somatosensory area) (a–h) and area Pv (the parietal ventral somatosensory area) (i–p) of the African wild dog. In all images, the pial surface is at the top of the image. Layer demarcations are provided in (c) for each cortical area. Scale bar in (p) = 250 μm and applies to all.

complement of five homologous cortical areas irrespective of phylogenetic history, current life history, brain size, and other factors that may potentially influence the number of cortical areas (Manger 2005).

In terms of the neurochemical aspects of the somatosensory system of the African wild dog, we can make a direct comparison to that described for the primary somatosensory cortex (area 3b) of the domestic dog (Hof et al. 1996), as we used four of the same antibodies (from the same manufacturers) in this study as used in the study of Hof et al. (1996)—these being those for neurofilament H, parvalbumin, calbindin, and calretinin. In area 3b of the domestic dog, Hof et al. (1996) report neurofilament H immunostaining in layers 3 and 5, with layer 3 showing a higher density of immunostained structures (soma and dendrites). In the African wild dog, we observed more immunopositive structures in layer 5, with very few structures labeled in layer 3 (Figure 10o). The pattern observed by Hof et al. (1996) for parvalbumin immunoreactivity—with the greatest density of labeled structures in layer 4, and lower densities in layers 3 and 5—is the same pattern observed in the African wild dog (Figure 10l). In the African wild dog, calbindin-immunopositive structures were

most dense in layer 2, with substantially lower densities in layers 3 and 5, and a distinct absence in layer 4 (Figure 10m). While the layer distribution of calbindin-immunopositive structures in the African wild dog is like that observed in the domestic dog, layer 4 of the domestic dog exhibited a high density of calbindin-immunopositive structures (Hof et al. 1996), which was absent in the African wild dog. The pattern of calretinin-immunopositive structures in the African wild dog and the domestic dog (Hof et al. 1996) was essentially similar, with both species exhibiting the highest density of structures in layer 2 and lower densities observed throughout layers 3–6. It is unclear how these differences in the presence/absence of neurofilament H and calbindin in the different cortical layers, when comparing the African wild dog and the domestic dog, will alter the processing of incoming somatosensory information in the cerebral cortex between these two canid species. The presence of calbindin in layer 4 neurons of the domestic dog area 3b, but not in layer 4 of the African wild dog, will alter the processing of incoming sensory information between species, which may play a role in the specificity with which tactile stimuli are perceived. Despite these differences, it is of interest to note that despite these differences, there are also many similarities. Thus, while the complement of cortical areas might be the same across carnivores, the neurochemistry of the cortex processing somatic information shows both similarities and variances, indicating that, perhaps at the species level, this neurochemistry might play a significant role in the differing manner in which species respond to tactile information.

4.2 | The Vestibular System of the African Wild Dog Compared to the Domestic Dog

To our knowledge, the only previous description of the vestibular system in the domestic dog is that provided by Singer (1962, plates 19 and 20), where he noted the presence of the lateral, medial, and superior vestibular nuclei, innervated by the vestibular branch of the vestibulocochlear nerve (8vn). In the African wild dog, we identified these three nuclei and the innervating nerve (8vn). In addition, we identified the magnocellular and parvocellular parts of the medial vestibular nucleus, as well as the vestibulocerebellar and spinal vestibular nuclei. It is highly likely that if the domestic dog brain was investigated in the same chemical neuroanatomical detail as done in the current study, these structures would be identified, as they are commonly observed in other carnivores and mammals (Highstein and Holstein 2006; Paxinos et al. 2009), including the related tree pangolin (Imam et al. 2019). It is therefore reasonable to conclude that the vestibular system of the African wild dog is likely to process vestibular information in a manner like that determined in other mammals. In addition, it is unlikely that the vestibular system plays any specific overt role in African wild dog sociality.

4.3 | No Apparent Sensory Specializations Related to Sociality of the African Wild Dog

This current study of the somatosensory and vestibular systems of the African wild dog completes our series of studies describing the major sensory systems in the African wild dog brain. It appears reasonable to conclude that, at the systems level of analysis, no overt specializations of the sensory systems are found, particularly in comparison to those reported in the domestic dog (e.g., Singer 1962). In the olfactory system, the potentially nuanced processing of semiochemicals in the accessory olfactory bulb may play an important role in the social behavior of African wild dogs, but not to an extent that would distinguish them from the role the accessory olfactory bulb plays in other canids (Chengetanai, Bhagwandin, et al. 2020a). For both the auditory (Chengetanai, Bhagwandin, et al. 2020b) and visual (Chengetanai, Bhagwandin, et al. 2020c) systems of the African wild dog, again, no overt specializations related to their reportedly complex social milieu (van den Berghe et al. 2019; Creel and Creel 2002) were observed. Thus, it appears most reasonable to conclude that the sociality of the African wild dog—specifically, the behaviors that are distinct to those observed in the domestic dog, such as aspects of their communication leading to collective decision-making (Walker et al. 2017; van den Berghe et al. 2019), is not primarily reliant on specializations of the sensory systems. This is not meant to indicate that these sensory systems do not play any role in social behavior, but rather that the neural processing underlying sociality in the African wild dog must occur in other regions of the brain. We are yet to investigate the motor, neuromodulatory, limbic, and cognitive systems of the African wild dog, and it is possible that a detailed analysis of all, or only some, of these regions of the African wild dog brain may reveal the neural underpinnings of the complex social behavior of this species.

Author Contributions

P.R.M. and M.A.S. conceptualized the study. M.F.B. and T.H obtained the brains. S.C., A.B., M.A.S., and P.R.M. performed the staining and analysis. S.C., P.R.H., M.A.S., and P.R.M. wrote the manuscript, and the remaining authors contributed to the editing and improvement of the early drafts of the manuscript. All authors had full access to all of the data in the study and take responsibility for the integrity of the data and the accuracy of the data analysis.

Acknowledgments

The authors have nothing to report.

Conflicts of Interest

Prof. Patrick Hof is an Editorial Board member of the *Journal of Comparative Neurology* and a co-author of this article. To minimize bias, he was excluded from all editorial decision-making related to the acceptance of this article for publication. The authors declare no other conflicts of interest.

Data Availability Statement

Data have not been shared due to this study being based on histological sections.

References

Berghänel, A., M. Lazzaroni, G. Cimarelli, S. Marshall-Pescini, and F. Range. 2022. "Cooperation and Cognition in Wild Canids." *Current Opinion in Behavioral Sciences* 46: 101173. https://doi.org/10.1016/j.cobeha.2022.101173.

Bertelsen, M. F. 2018. "Issues Surrounding Surplus Animals in Zoos." In *Fowler's Zoo and Wild Animal Medicine, Current Therapy*. Vol. 9, edited by R.E. Miller N. Lamberski, and P. Calle, 134–137. Elsevier.

Celio, M. R. 1990. "Calbindin D-28k and Parvalbumin in the Rat Nervous System." *Neuroscience* 35: 375–475. https://doi.org/10.1016/0306-4522(90)90091-h.

Chengetanai, S., A. Bhagwandin, M. F. Bertelsen, et al. 2020a. "The Brain of the African Wild Dog. II. The Olfactory System." *Journal of Comparative Neurology* 528: 3285–3304. https://doi.org/10.1002/cne.25007.

Chengetanai, S., A. Bhagwandin, M. F. Bertelsen, et al. 2020b. "The Brain of the African Wild Dog. III. The Auditory System." *Journal of Comparative Neurology* 528: 3229–3244. https://doi.org/10.1002/cne.24989.

Chengetanai, S., A. Bhagwandin, M. F. Bertelsen, et al. 2020c. "The Brain of the African Wild Dog. IV. The Visual System." *Journal of Comparative Neurology* 528: 3262–3284. https://doi.org/10.1002/cne.25000.

Chengetanai, S., J. Tenley, M. F. Bertelsen, et al. 2020. "The Brain of the African Wild Dog. I. Anatomy, Architecture, and Volumetrics." *Journal of Comparative Neurology* 528: 3245–3261. https://doi.org/10.1002/cne.24999.

Claase, M. J., M. I. Cherry, W. McNutt, P. J. Apps, and N. R. Jordan. 2024. "Size Matters: Natural Experiments Suggest the Dear Enemy Effect Is Moderated by Pack Size in African Wild Dogs." *Ecology and Evolution* 14: e11298. https://doi.org/10.1002/ece3.11298.

Clemo, H. R., and M. A. Meredith. 2004. "Cortico-Cortical Relations of Cat Somatosensory Areas SIV and SV." *Somatosensory and Motor Research* 21: 199–209. https://doi.org/10.1080/08990220400012505.

Clemo, H. R., and B. E. Stein. 1983. "Organization of a Fourth Somatosensory Area of Cortex in Cat." *Journal of Neurophysiology* 50: 910–925. https://doi.org/10.1152/jn.1983.50.4.910.

Creel, S., and N. M. Creel. 2002. *The African Wild Dog. Behavior, Ecology, and Conservation*. Princeton University Press.

Foxworthy, W. A., and M. A. Meredith. 2011. "An Examination of Somatosensory Area SIII in Ferret Cortex." *Somatosensory and Motor Research* 28: 1–10. https://doi.org/10.3109/08990220.2010.548465.

Gallyas, F. 1979. "Silver Staining of Myelin by Means of Physical Development." *Neurological Research* 1: 203–209. https://doi.org/10.1080/01616412.1979.11739553.

Griffin, G. D., S. L. Ferri-Kolwicz, B. A. S. Reyes, E. J. van Bockstaele, and L. M. Flanagan-Cato. 2010. "Ovarian Hormone-Induced Reorganization of Oxytocin-Labeled Dendrites and Synapses Lateral to the Hypothalamic Ventromedial Nucleus in Female Rats." *Journal of Comparative Neurology* 518: 4531–4545. https://doi.org/10.1002/cne.22470.

Guran, C. N. A., M. Boch, R. Sladky, et al. 2024. "Functional Mapping of the Somatosensory Cortex Using Noninvasive fMRI and Touch in Awake Dogs." *Brain Structure and Function* 229: 1193–1207. https://doi.org/10.1007/s00429-024-02798-0.

Highstein, S. M., and G. R. Holstein. 2006. "The Anatomy of the Vestibular Nuclei." *Progress in Brain Research* 151: 157–203. https://doi.org/10.1016/S0079-6123(05)51006-9.

Hof, P. R., Y. E. Bogaert, R. E. Rosenthal, and G. Fiskum. 1996. "Distribution of Neuronal Populations Containing Neurofilament Protein and Calcium-Binding Proteins in the Canine Cortex: Regional Analysis and Cell Typology." *Journal of Chemical Neuroanatomy* 11: 81–98. https://doi.org/10.1016/0891-0618(96)00126-3.

Imam, A., A. Bhagwandin, M. S. Ajao, M. A. Spocter, and P. R. Manger. 2019. "The Brain of the Tree Pangolin (*Manis tricuspis*). VI. The Brainstem and Cerebellum." *Journal of Comparative Neurology* 527: 2440–2473. https://doi.org/10.1002/cne.24721.

Jones, E. G. 2007. *The Thalamus*. Cambridge University Press.

Kaas, J. H. 2012. "Somatosensory System." In *The Human Nervous System*, 3rd ed., edited by J. K. Mai and G. Paxinos, 1074–1109. Academic Press. https://doi.org/10.1016/B978-0-12-374236-0.10030-6.

Kaiser, A., O. Alexandrova, and B. Grothe. 2011. "Urocortin-Expressing Olivocochlear Neurons Exhibit Tonotopic and Developmental Changes in the Auditory Brainstem and in the Innervation of the Cochlea." *Journal of Comparative Neurology* 519: 2758–2778. https://doi.org/10.1002/cne.22650.

Laux, A., F. Delalande, J. Mouheiche, et al. 2012. "Localization of Endogenous Morphine-Like Compounds in the Mouse Spinal Cord." *Journal of Comparative Neurology* 520: 1547–1561. https://doi/org/10.1002/cne.22811.

Liu, X., H. Huang, T. P. Snutch, P. Cao, L. Wang, and F. Wang. 2022. "The Superior Colliculus: Cell Types, Connectivity, and Behavior." *Neuroscience Bulletin* 38: 1519–1540. https://doi.org/10.1007/s122w64-022-00858-1.

Manger, P. R. 2005. "Establishing Order at the System Level in Mammalian Brain Evolution." *Brain Research Bulletin* 66: 282–289. https://doi.org/10.1016/j.brainresbull.2005.05.002.

Manger, P. R., M. G. P. Rosa, and R. Collins. 2001. "Somatotopic Organization and Cortical Projections of the Ventrobasal Complex of the Flying Fox: An "Inverted" Wing Representation in the Thalamus." *Somatosensory & Motor Research* 18: 19–30. https://doi.org/10.1080/08990220020002079.

Maseko, B. C., N. Patzke, K. Fuxe, and P. R. Manger. 2013. "Architectural Organization of the African Elephant Diencephalon and Brainstem." *Brain, Behavior and Evolution* 82: 83–128. https://doi.org/10.1159/000352004.

McGreevy, P. D., D. Georgevsky, J. Carrasco, M. Valenzuela, D. L. Duffy, and J. A. Serpell. 2013. "Dog Behavior Co-Varies With Height, Bodyweight and Skull Shape." *PLoS ONE* 8: e80529. https://doi.org/10.1371/journal.pone.0080529.

Ngwenya, A., N. Patzke, P. R. Manger, and S. Herculano-Houzel. 2016. "Continued Growth of the Central Nervous System Without Mandatory Addition of Neurons in the Nile Crocodile (*Crocodylus niloticus*)." *Brain, Behavior and Evolution* 87: 19–38. https://doi.org/10.1159/000443201.

Norrsell, U. 1978. "Sensory Defects Caused by Lesions of the First (SI) and Second (SII) Somatosensory Areas of the Dog." *Experimental Brain Research* 32: 181–195. https://doi.org/10.1007/BF00239726.

Paxinos, G., C. Watson, P. Carrive, M. T. K. Kirkcaldie, and K. Ashwell. 2009. *Chemoarchitectonic Atlas of the Rat Brain*. Elsevier.

Piskuric, N. A., C. Vollmer, and C. A. Nurse. 2011. "Confocal Immunofluorescence Study of Rat Aortic Body Chemoreceptors and Associated Neurons *In Situ* and *In Vitro*." *Journal of Comparative Neurology* 519: 856–873. https://doi.org/10.1002/cne.22553.

Sawyer, E. K. 2017. "Conserved Patterns of Trigeminal Somatosensory System Organization in Mammals." *Brain, Behaviour and Evolution* 89: 65–67. https://doi.org/10.1159/000460812.

Sawyer, E. K., and D. K. Sarko. 2017. "Comparative Anatomy and Evolution of the Somatosensory Brain Stem." In *Evolution of Nervous Systems*. 2nd ed., Vol. 2, edited by J. H. Kaas, 437–458. Elsevier.

Sawyer, E. K., E. C. Turner, and J. H. Kaas. 2016. "Somatosensory Brainstem, Thalamus, and Cortex of the California Sea Lion (*Zalophus californianus*)." *Journal of Comparative Neurology* 524: 1957–1975. https://doi.org/10.1002/cne.23984.

Schroder, D. M., and J. A. Jane. 1976. "The Intercollicular Area of the Inferior Colliculus." *Brain, Behavior and Evolution* 13: 125–141. https://doi.org/10.1159/000123805.

Schwaller, B., I. Durussel, D. Jermann, B. Herrmann, and J. A. Cox. 1997. "Comparison of the Ca2+-Binding Properties of Human Recombinant Calretinin-22k and Calretinin." *Journal of Biological Chemistry* 272: 29633–29671.

Schwark, H. D., H. Esteky, and E. G. Jones. 1992. "Corticocortical Connections of Cat Primary Somatosensory Cortex." *Experimental Brain Research* 91: 425–434. https://doi.org/10.1007/BF00227839.

Singer, M. 1962. *The Brain of the Dog in Section*. W.B. Saunders Company.

Sternberger, L. A., and N. H. Sternberger. 1983. "Monoclonal Antibodies Distinguish Phosphorylated and Nonphosphorylated Forms of Neurofil-

aments *In Situ*." *Proceedings of the National Academy of Science of the United States of America* 80: 6126–6130. https://doi.org/10.1073/pnas.80.19.6126.

ten Donkelaar, H. J., J. Broman, and P. van Domburg. 2020. "The Somatosensory System." In *Clinical Neuroanatomy. Brain Circuitry and Its Disorders*, edited by H. J. ten Donkelaar, 171–255. Springer Nature. https://doi.org/10.1007/978-3-030-41878-6_4.

van den Berghe, F., M. C. J. Paris, Z. Sarnyai, et al. 2019. "Dog Appeasing Pheromone Prevents the Androgen Surge and May Reduce Contact Dominance and Active Submission After Stressful Interventions in African Wild Dogs (*Lycaon pictus*)." *PLoS ONE* 14: e0212551. https://doi.org/10.1371/journal.pone.0212551.

Walker, R. H., A. J. King, J. W. McNutt, and N. R. Jordan. 2017. "Sneeze to Leave: African Wild Dogs (*Lycaon pictus*) Use Variable Quorum Thresholds Facilitated by Sneezes in Collective Decisions." *Proceedings of the Royal Society B: Biological Sciences* 284: 20170347. https://doi.org/10.1098/rspb.2017.0347.

Ward, C., E. B. Bauer, and B. B. Smuts. 2008. "Partner Preferences and Asymmetries in Social Play Among Domestic Dog, *Canis lupus familiaris*, Littermates." *Animal Behaviour* 76: 1187–1199. https://doi.org/10.1016/j.anbehav.2008.06.004.

Willis, W. D., and K. N. Westlund. 1997. "Neuroanatomy of the Pain System and the Pathways That Modulate Pain." *Journal of Clinical Neurophysiology* 14: 2–31. https://doi.org/10.1097/00004691-199701000-00002.

Wong, P., O. A. Gharbawie, L. E. Luethke, and J. H. Kaas. 2008. "Thalamic Connections of Architectonic Subdivisions of Temporal Cortex in Grey Squirrels (*Sciurus carolinensis*)." *Journal of Comparative Neurology* 510: 440–461. https://doi.org/10.1002/cne.21805.